Semimetal-semiconductor Transitions in Bismuth-antimony Films and Nanowires Induced by Size Quantization

A. A. Nikolaeva[a,b], L. A. Konopko[a,b], V. M. Grabov[c], V. A. Komarov[c], N. Kablukova[c], Gh. I. Para[a], I. A. Popov[a]

[a]Ghitu Institute of Electronic Engineering and Nanotechnologies, ASM, 3/3, Academiei, str., Chisinau, MD-2028, Republic of Moldova, e-mail: A.Nikolaeva@nano.asm.md
[b]International Laboratory of High Magnetic Fields and Low Temperatures, 95, Gajowicka, str., Wroclaw, 53-421, Poland
[c]Herzen State Pedagogical University, 6, Kazanskaya (Plekhanova), str., St. Petersburg, 191186, Russia

In this paper we present the experimental results of an investigation of the electrical transport, thermoelectrical properties, the Shubnikov de Haas oscillations of $Bi_{1-x}Sb_x$ films ($0 < x < 0.04$) grown by the vacuum thermal evaporation and nanowires prepared by a modified Ulitovsky – Teilor technique. The results of the X-ray diffraction indicate that the trigonal axes were perpendicular to the film plane and the single Bi-2at%Sb nanowires with the diameter 100–1000 nm were represented by single crystals in a glass capillary with (1011) orientation along the wire axis. The investigations of the Shubnikov de Haas oscillations on Bi-2at%Sb wires with $d > 600$ nm show that overlapping of L and T bands was twice smaller than that in pure Bi. The temperature dependences of thin semimetalic Bi-3at%Sb films and Bi-2at%Sb wires show a semiconducting behavior. The semimetal-semiconductor transition induced by the quantum confinement effect is observed in semimetal $Bi_{1-x}Sb_x$ films and nanowires at the diameters up to five times greater than those in the pure Bi. That experimental fact, on the one hand, will allow observing the display quantum confinement effect at higher temperatures on nanowires of the same diameters, and, on the other hand, will allows separating effects connected with the surface state and the quantum size effects. In addition, the thermoelectric properties and thermoelectric efficiency of bismuth-antimony wires are considered and a possibility to use them in thermoelectric converters of energy is discussed.

Keywords: nanowires, films, semimetal-semiconductor transition, size quantization, thermoelectricity.

УДК 539.261.1

INTRODUCTION

Semimetals and narrow band gap semiconductors have received particular attention because of their physical properties of interest for both fundamental physics and engineering of materials. It is known that best materials for thermoelectric and magnetothermoelectric cooling at the temperature as low as 100 K are $Bi_{1-x}Sb_x$ alloys which have also been the subject of many experimental investigations [1–4]. Those studies clearly indicate that the $Bi_{1-x}Sb_x$ alloys have a great potential to be used in solid state cooling devices to attain low temperatures.

The thermoelectric efficiency depends on the thermoelectric figure of merit of the thermoelectric material of which the thermoelectric device is made. The figure of merit (ZT) of the materials is given by:

$$ZT = \frac{\sigma\alpha^2}{\chi}T, \qquad (1)$$

where σ is the electrical conductivity, α – the Seebeck coefficient, the total thermal conductivity $\chi = \chi_e + \chi_p$, (χ_e is the electronic thermal conductivity, χ_p is the lattice thermal conductivity), and T is the absolute temperature [5].

Searching for high ZT materials is essential in thermoelectric power generation and refrigeration.

One way to increase ZT is to maximize the Power factor $\alpha^2\sigma$ for a given χ through optimizing the electronic band structure of the material. One approach for increasing Z is to search for physical systems exhibiting an enhanced thermoelectric power. The authors in [6–8] showed that due to the quantum-mechanical nature of the motion of electrons in low dimensional structure, an enhancement of ZT should result.

It has been predicted [9] that the thermoelectric efficiency of semimetalic $Bi_{1-x}Sb_x$ nanowires ($0 < x < 0.04$) can be significantly enhanced relative to Bi nanowires [6–8].

When bismuth is alloyed with antimony the band structure is strongly affected. The direct gap at the L point decreases up to $x = 0.04$, where the L bands invert and the direct gap then increases with increasing the antimony content. The semimetal-semiconductor transition is around $x = 0.07$ and the semiconductor-semimetal transition occurs at $x = 0.22$.

Since the overlapping of L and T bands in semimetal $Bi_{1-x}Sb_x$ alloys is smaller than of those in pure Bi, the quantum confinement effects and in particu-

lar semimetal-semiconductor transition in $Bi_{1-x}Sb_x$ nanowires and films can be observed at much larger diameters than in pure Bi nanowires. On the one hand, it simplifies the manufacturing technology of single-crystal quantum wires and application of methods to control their diameters. On the other hand, this will make it possible to separate the effects related to the size quantization and to the surface state, which were not taken into account in theoretical works [6–9] but play an important role in Bi wires with $d \sim 50$ nm [10, 11].

Therefore, we expect to obtain higher values of thermoelectric efficiency at larger diameters in $Bi_{1-x}Sb_x$ nanowires as compared to those in Bi nanowires.

To preserve quasi-discrete nature of the spectrum during manifestation of the quantum size effects, it is necessary for the broadening h/τ (τ – relaxation time) to be shorter than the distance between adjacent subbands $h/\tau << \varepsilon_{s+1} - \varepsilon_s$. Thus, for the manifestation of the confinement effect, the most stringent requirement is purity and exceptionally high structural perfection of single-crystal nanowires or films.

The quantum size effect, which appears in the oscillatory dependence of $R(d)$, as well as the Hall effect $R(d)$ and the mobility $\mu(d)$ were observed at low and room temperatures in Bi and $Bi_{1-x}Sb_x$ films thermally sprayed onto various substrates [12–14]. A small step in the aforementioned oscillating thickness dependence does not allow conducting similar studies in thin wires.

A suitable material for studies of the influence of the quantum size effects on thermopower and resistance are single-crystal nanowires of $Bi_{1-x}Sb_x$ ($0 < x < 0.04$) in a glass capillary prepared by the high frequency liquid phase casting [15–17], and monocrystalline Bi-3at%Sb films prepared by thermal spraying on the mica substrate with subsequent recrystallisation under cover [18].

Here we report the experimental temperature dependent resistance and thermopower of $Bi_{1-x}Sb_x$ nanowires and films with different diameters in the semimetal region and investigate the singularity of the manifestation of the dimensional effect in the temperature range of 4.2–300 K and in the magnetic field up to 14 T.

SAMPLES AND EXPERIMENT

A textured bismuth-antimony Bi-3at%Sb films were prepared by discrete thermal evaporation in vacuum (10^{-5} mm Hg.) on a substrate at the temperature of 410 K. Muscovite mica and a polyimide film were used as substrates. After deposition, the films were annealed at 540 K. The choice of material for substrates was mostly for two reasons. Mica has a crystalline structure, which has an orienting effect on a bismuth film and bismuth-antimony solid solutions, so that the orientation of crystallites of the films is usually characterized by the C_3 axis perpendicular to the substrate plane. A polyimide substrate is amorphous, but the film grows with the same orientation of the C_3 axis as it grows on a mica substrate.

The coefficient of linear thermal expansion of mica, bismuth, and polyimide is $(7.5–8.5)\cdot10^{-6}$ K^{-1} < $11\cdot10^{-6}$ K^{-1} < $(30–50)\cdot10^{-6}$ K^{-1}, respectively. Therefore, at a temperature below the temperature of formation of the film, the film tests the planar elongation in case of the mica substrate and planar compression in case of a polyimide substrate.

To obtain monocrystalline bismuth and bismuth antimony films the method of zone recrystallization under cover was used [18]. The essence of the method is as follows: on the original substrate, containing a depozited Bi or $Bi_{1-x}Sb_x$ film, the protective cover – KBr layer is sprayed. Thus, the film is in the container. The protective coating is needed to prevent contraction of the film into droplets and to avoid any interaction of the molten material with the atmosphere. The inert atmosphere was produced by nitrogen purge.

Then this container was put into the installation for zone recrystallization. The temperature recrystallization was 290–300°C, the zone width 1–1.5 mm and the velocity recrystallization $v = 2$ cm/h. After recrystallization the KBr cover has been removed by dissolution in water.

The structure of the films was analyzed by the X-ray diffraction using the rotating crystal method in compliance with the Wolf-Bragg focusing. This method provides a possibility to determine the orientation of the planes relative to the substrate plane and, additionally, control the composition of the film.

The results of the X-ray diffraction studies of $Bi_{1-x}Sb_x$ films ($x = 0.03$) are shown in Fig. 1.

A small width of the diffraction peaks of the film as well as a good resolution of the X-ray peak of the doublet in the fifth order confirm the perfection of the crystal structure of the films and indicate a uniform distribution of antimony over the film.

To provide the absence of block boundaries in the internal structure, the film is subjected to etching with the subsequent analysis of etch pits by the optical and atomic force microscopy. Since the sizes of the film (2 mm x 10 mm) are considerably larger than the maximal possible view in the atomic force microscopy, optical microscopy is a more informative method.

The etch pits are mirror images of the crystal orientation in the C_1C_2 basal plane and confirm that the

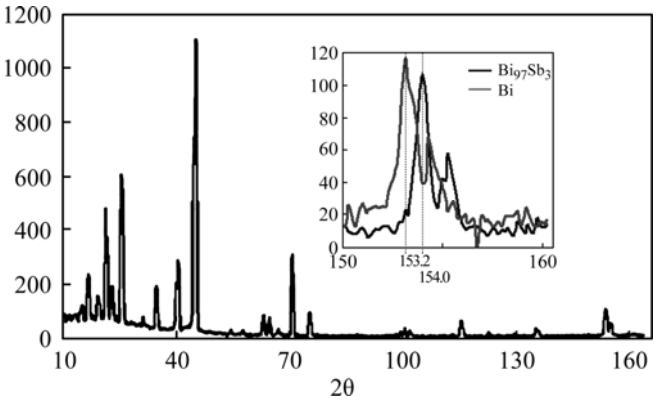

Fig. 1. X-ray diffraction pattern of Bi-3at%Sb film on mica. Inset: fifth-order peak of Bi and Bi-3at%Sb.

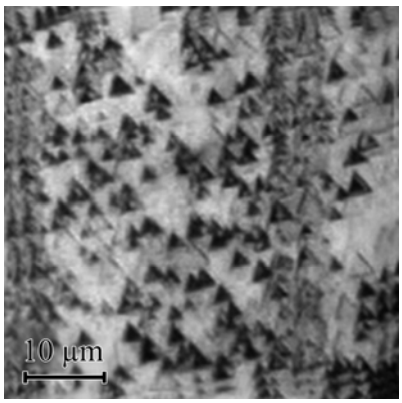

Fig. 2. Optical microscopy image of 50 μm single-crystal film after etching.

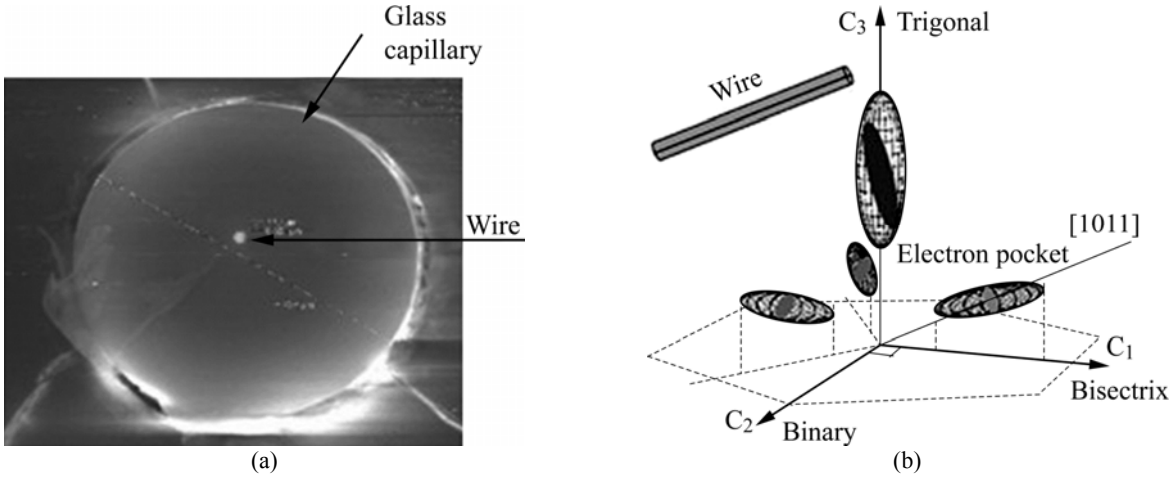

Fig. 3. SEM cross sectional image: (a) of 650 nm Bi-2at%Sb wire (clear) in glass envelope (gray); (b) schematic diagrams of the Fermi surface electrons and holes relative to the main crystallographic direction and orientation of Bi wire. Extreme of the Fermi surface, *L* electrons, and *T* holes in the direction perpendicular to the wire axis are shaded.

film is single-crystal and (111) is oriented perpendicular to the film plane (Fig. 2).

Individual monocrystalline Bi-2at%Sb nanowires in a glass cover with different diameters were fabricated by the high frequency liquid phase casting (Ulitovsky-Taylor method) [16, 17]. The length of the wires was more than 1–2 mm. Multiple horizontal zone recrystallization of the nanowires was used for the homogenization of wires and for the improvement of their structural perfection. At v_z = 0.1 mm/h, $Bi_{1-x}Sb_x$ wires are seen to be homogeneous. Electrical and thermal contacts to the nanowires were prepared using $In_{0.5}Ga_{0.5}$ eutectics just before measurements to prevent the diffusion of In or Ga in the sample.

Figure 3a shows the SEM image of the $Bi_{1-x}Sb_x$ wire in a glass capillary. The wires had a strictly cylindrical shape. The glass envelope was very close to the wire surface and was more than an order of magnitude greater than the wire diameter.

The test measurements of the crystallographic orientation of the wires were carried out using an Xcalibur-E Diffractometer; they show that their principal axes are oriented along the (1011) crystallographic direction.

The measurement the angular rotation diagrams transverse [$H \perp I$] magneto-resistance (ADTMR) $R(\theta)$ and Shubnikov de Haas (SdH) oscillations have allowed to conclude that $Bi_{1-x}Sb_x$ wires of all diameters had the same orientation (1011) along the wire axes. In this case the wire axes make an angle of about 19° with the bisector axis C_1 in the bisector-trigonal plane C_1; C_3 and the binary axis C_2 are perpendicularly to the wire axis (Fig. 3b).

Figure 4 shows the ADTMR $\Delta R/R(\theta)$ in the trigonal-binary plane in a constant magnetic field H = 0.4 T, perpendicular to the current Bi-2at%Sb wires with different diameters at 300 K. As clearly seen in Fig. 4, all curves are symmetric with respect to the C_2 axis (θ = 90°). At θ = 0, the magnetic field H is close to the direction at which H is parallel to the C_3 axis. When decreasing the wire diameter d, the anisotropy of the magnetoresistance decreases.

Using the ADTMR $R(\theta)$, ($H \perp I$), the wire was oriented in a magnetic field so that the magnetic field vector $\vec{H}$ coincided with certain crystallographic axes C_2 and C_3 of the wires.

The galvanomagnetic and thermoelectric coefficients were measured in the temperature range

4.2–300 K in magnetic fields up to 14 T in the main crystallographic orientation.

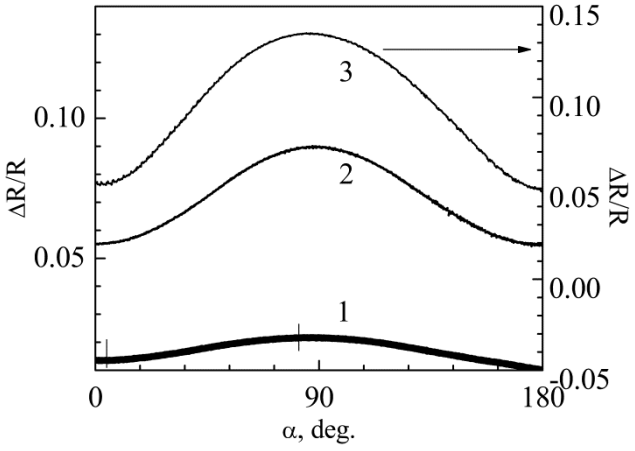

Fig. 4. Angular dependences of residual magnitoresistance in the trigonal-binary plane in constant magnetic field H = 0.4 T ($H \perp I$), Bi-2at%Sb nanowires of different diameters: 1 – d = 300 nm; 2 – d = 600 nm; 3 – d = 900 nm; T = 300 K.

The investigation of the SdH oscillations in Bi and Bi-2%Sb wires was carried out in magnetic fields up to 14 T at liquid helium temperatures and at 1.5 K on a setup, which permitted automatic recording of the resistance $R(H)$ and $\partial R/\partial H(H)$ curves at $H \parallel I$ and $H \perp I$.

Measurements in a strong magnetic field were performed in the International Laboratory of High Magnetic Fields and Low Temperatures (Wroclaw, Poland).

RESULTS AND DISCUSSION

The SdH oscillations from both light electrons at L and holes at T in all Bi-2at%Sb wires with $d > 300$ nm were observed.

Oscillatory dependences recorded in both the longitudinal ($H \parallel I$), and the transverse magnetic fields ($H \parallel C_3$ and $H \parallel C_2$), which in each case allowed recovering the form of the electron and the hole Fermi surface in L and T points of the Brillouin zone. For comparison, Fig. 5 shows the SdH oscillations in $H \parallel C_2$ ($H \perp I$) direction of pure Bi (curve *1*) and Bi-2at%Sb wires (curves *2*, *3*).

In this orientation, in a weak magnetic field, the oscillations from two equal mean main cross sections of the Fermi surface at L are observed. In strong magnetic fields, the oscillations from the maximum section $S^T_{\max}$ of holes in T have been observed. The regions of existence of the SdH oscillations from L electrons and T holes are separated in the magnetic field due to a significant difference in the extreme section FS of L electrons and T holes in this direction. Displacement of a field of a quantum limit of the SdH oscillations both from $L_{2,3}$ electrons and T holes in the area of a weak magnetic field is a clear evidence of a decrease of the Fermi surface in Bi-2at%Sb wires in comparison with those in pure Bi wires.

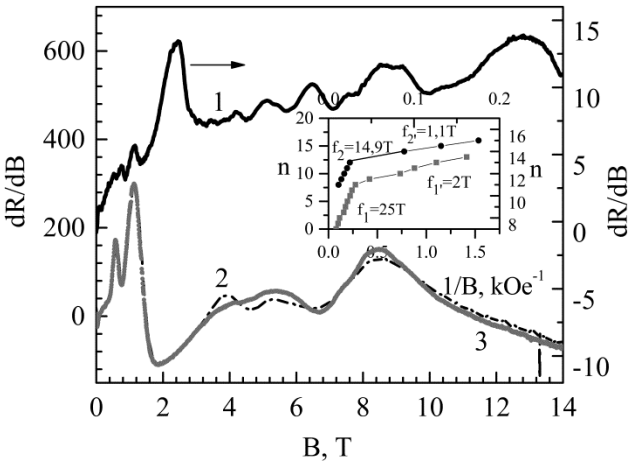

Fig. 5. SdH oscillation in Bi and Bi-2%Sb wires on derivative TMR $\partial\rho/\partial H(H)$, $H \perp I$, $H \parallel C_2$. Inset: dependences of quantum number of SdH oscillations from inverse magnetic field $1/H$. 1 – pure Bi wire; 2 – T = 4.2 K; 3 – T = 2.1 K for Bi-2at%Sb, d = 600 nm.

The frequency of the SdH oscillations $f_2 = 1/\Delta\,(H)$ from the maximum cross-section of the T hole ellipsoid decreases from 25 T to 14.9 T for pure Bi and Bi-2at%Sb wires. The frequency of the SdH oscillations from two equivalent electronic ellipsoids $L_{2,3}$ decreased almost 2-fold: from f_1 = 2 T to f_2 = 1,1 T.

To estimate the changes of overlapping of L and T bands by adding Sb in Bi, the well-known expressions were used, allowing for definition of the energy position of the Fermi level for L and T electrons and holes [19].

The values of the Fermi level of the holes and electrons ε_F^h and ε_F^e were calculated according to expressions (1–3):

$$\varepsilon_F^T = \varepsilon_{par} - \frac{1}{2}\varepsilon_g^T + \left[\varepsilon_{par}^2 + \left(\frac{1}{2}\varepsilon_{gT}\right)^2\right]^{\frac{1}{2}} \qquad (1)$$

where ε_{par} is the energy in the parabolic band approximation, ε_F^T is holes of the Fermi energy (FE) in the T point, m_c^T is the minimum cyclotron mass of T holes; $\varepsilon_g^T = 200$ meV is the gap in the T point of the Brillouin zone, Δ_T^{-1} – frequency of the SdH oscillations from the minimum cross section of the Fermi surface (FS) T – holes at $H \parallel C_3$.

$$\varepsilon_{par} = \frac{S_T}{2\pi m_c^T} = \frac{eh \cdot \Delta_T^{-1}}{2\pi c \cdot m_c^T}. \qquad (2)$$

The FL of the electrons in the L point is:

$$\varepsilon_F^e = \frac{eh}{2\pi} \times \frac{\Delta_e^{-1}}{m_c^e}. \quad (3)$$

Cyclotron masses of electrons and holes on the Fermi level were determined from the temperature dependence of the amplitude of the SdH oscillations at $H \parallel C_2$ (Fig. 5, curves *2*, *3*).

The Dingle temperature T_D determined from the dependence of the amplitude of the SdH oscillations in the magnetic field was 2 K, which indicates a high structural perfection of Bi-2at% Sb wires in a glass insulation.

The values of the cyclotron masses, the Dingle temperature and ε_F in the pure Bi and Bi-2at%Sb wires, calculated from the SdH oscillations, are presented below for comparison:

$pure-\mathrm{Bi}$	$\mathrm{Bi}-2\mathrm{at\%Sb}$
$f_{2,3} = 3T$	$f_{2,3} = 2T$
$m_L^e = 0.01m_0, T_D = 1\,\mathrm{K}$	$m_L^e = 0.01m_0, T_D = 2\,\mathrm{K}$
$m_h^h = 0.22m_0$	$m_h^h = 0.19m_0$
$E^h{}_F = 12\,\mathrm{meV}$	$E^h{}_F = 9\,\mathrm{meV}$
$E_F^e = 30\,\mathrm{meV}$	$E_F^e = 13\,\mathrm{meV}$
$E_{ov} = 42\,\mathrm{meV}$	$E_{ov} = 21\,\mathrm{meV}$

Using m_c^T, m_c^e and Δ_T^{-1}, Δ_e^{-1} from the SdH oscillations and expressions (1–3), the values of $E^h{}_f = 9$ meV and $E^e{}_F = 13$ meV, respectively, have been calculated.

Thus the overlapping of L and T bands decreases up to $E_{ov} = 21$ meV, which is almost twice less than in the pure Bi wires. So, really the semimetal-semiconductor transition in Bi-2at%Sb wires can occur at larger diameters than in pure Bi.

Figure 6 shows the temperature dependences of the resistivity $R(T)$ of the Bi-3at%Sb films of two different thicknesses deposited on mica (a) and polyimide (b) substrates. Figure 7 shows the temperature dependences of the residual resistance $\Delta R/R(T) = (R_T - R_0)/R_0(T)$ of Bi-2at%Sb wires with different diameters.

The gap ε_g was determined from the temperature dependence of the resistivity of the inverse temperature. Figures 6a and b (insets) show the dependences of the resistivity $\rho(10^3/T)$, which permits determination of the gap $\varepsilon_g{}^L$, T in films.

In the range of temperatures $T > 100$ K on dependences $\rho(10^3/T)$ it is possible to allocate a linear curve pieces. On inclination of these pieces, according to the expression $\rho = \rho_0 \exp\left(-\frac{\Delta E}{2\kappa T}\right)$, it was possible to calculate the energy gap width ε_g and its dependence on the diameter and a substrate kind.

The maximum value of ε_g = 30 meV for Bi-3at%Sb films (d = 300 nm), deposited on mice and the minimum value of ε_g = 7 meV for a Bi-3at%Sb deposited on polyimide were obtained.

On the one hand, it is because in Bi-3at%Sb films the overlapping of L and T bands ε_{ov} is less than in Bi-2at%Sb. On the other hand, the compressing action of mica and the stretching action of polyimide on the substrate lead to the maximal value of ε_g on the films deposited on mica and the minimal value of ε_g on the films with polyimide substrate.

For both films and wires the substantial temperature dependence of $R(T)$ on the thickness was observed.

In Bi-2at%Sb wires the semimetal-semiconductor transition is observed at d < 500 nm, while in the Bi-3at%Sb films the semiconductor dependence $R(T)$ remain till the thickness becomes 1000 nm (Figs. 6a,b, curves *2*). In Bi-2at%Sb wires with d = 200 nm, the resistance $R(T)$ increases 3.5 times.

In the temperature range of 4.2–300 K at Bi-3at%Sb films with the diameter of 300 nm deposited on mica the resistance $R(T)$ increases 6–7 times (Fig. 6), and on a substrate from polyimide the resistance $R(T)$ increases 3–4 times. Besides, unlike Bi-2at%Sb wires, the resistance $R(T)$ 1000 nm of films on mica and polyimide substrate also increases 2.2 and 1.6 times, respectively.

On the one hand due to the fact that in the Bi-3at%Sb alloy the overlap T and L bands is less, compared with the Bi-2at%Sb and on the other hand in the deposited on the mica films observed of "compression" effect in the direction perpendicular to the film plane, which, also leads to a reduction of overlap of L and T bands, the highest value of the gap ε_g = 30 meV in Bi-3at%Sb films on the mica substrate (d = 300 nm) has been observed.

Simultaneously with the measurements of the temperature dependence of $R(T)$ the measurements of temperature dependences of thermopower $\alpha(T)$ have been made in Bi-2at%Sb wires with different diameters (Fig. 8). In thin wires at temperatures < 150 K the thermopower changes its sign and forms a peak of a positive polarity in which α reaches +150 μV/K at T = 35–40 K.

As well as in pure bismuth wires, with decreasing of wires diameter a point of change of a sign of thermopower and the peak positive (+) polarity on temperature dependence $\alpha(T)$ are displaces in the high temperature area.

It is known that in Bi crystals the thermopower is determined by contribution of electrons in the conduction band in the L point and of holes in the T point of the Brillouin zone.

According to [20], the diffusion thermopower in the case of two types of carriers looks like:

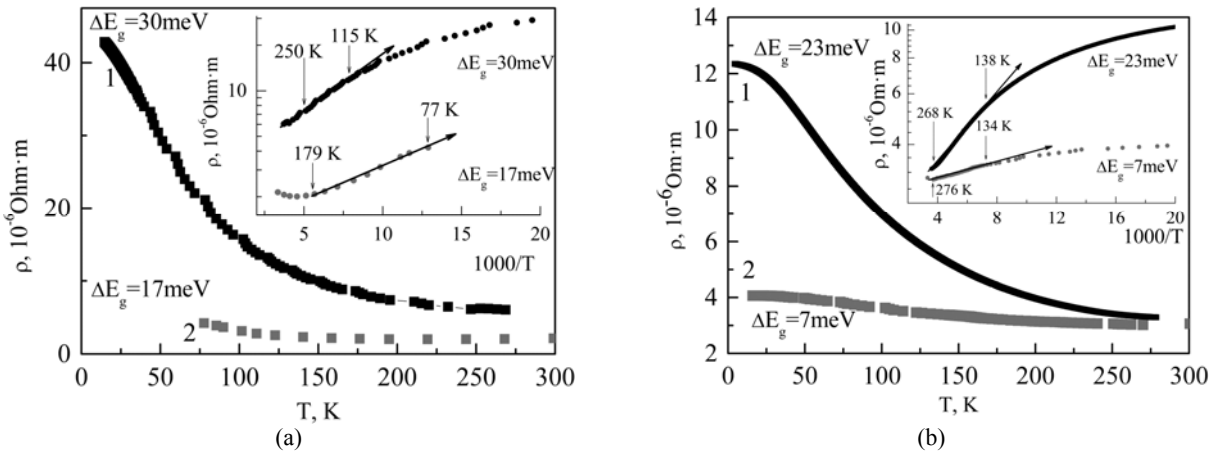

Fig. 6. Experimental temperature dependences of resistivity $\rho(T)$ of Bi-3at%Sb films, deposited on mica (a) and polyimide (b). Inset: dependences of $\rho(10^3/T)$ on thickness of film: 1 – d = 300 nm; 2 – d = 1000 nm.

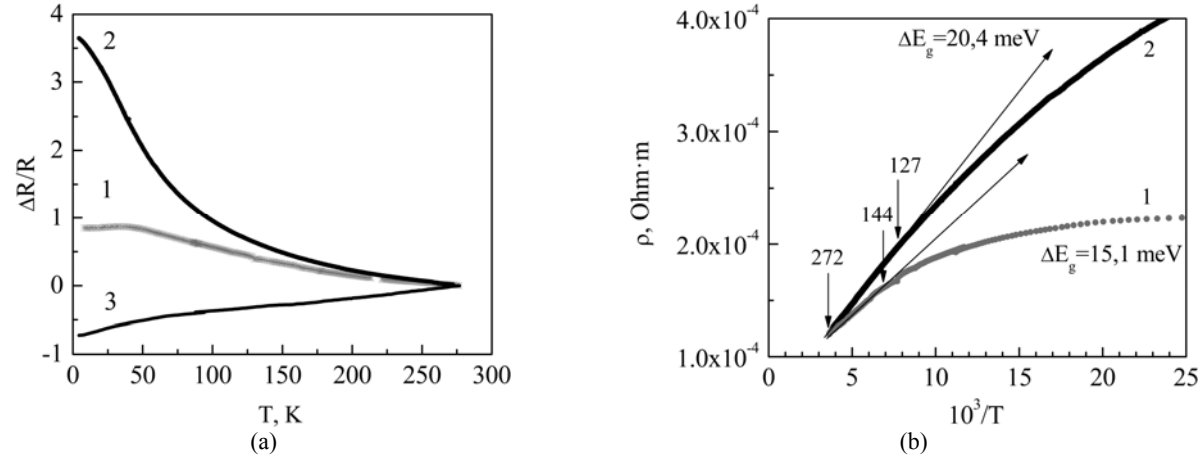

Fig. 7. Experimental temperature dependences of residual resistance $\Delta R/R(T)$ in Bi-2at%Sb wires: 1 – d = 200 nm; 2 – d = 500 nm; 3 – d = 1600 nm (a) and (b) dependences $\rho(10^3/T)$.

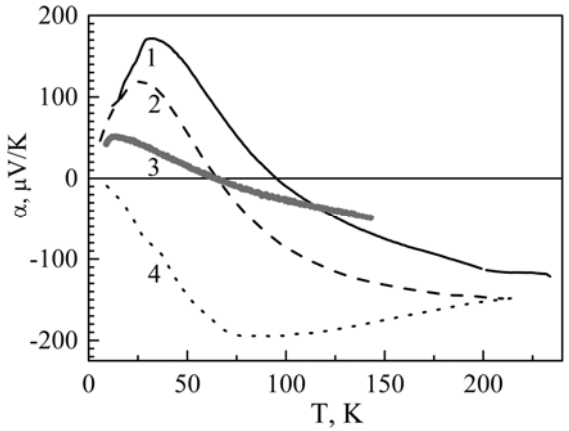

Fig. 8. Temperature dependences of thermopower $\alpha(T)$ for Bi-2at%Sb wires with various diameters d: 1 – d = 300 nm; 2 – d = 400 nm; 3 – d = 600 nm; 4 – d = 1600 nm.

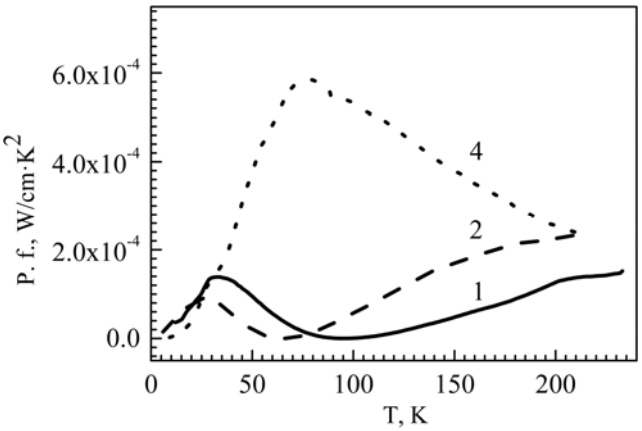

Fig. 9. Temperature dependences of Power factor = $\alpha^2\sigma(T)$ for Bi-2at%Sb wires, T = 26 K, at various diameters d: 1 – d = 300 nm; 2 – d = 400 nm; 4 – d = 1600 nm.

$$\alpha = \frac{\alpha_L(\sigma_{L1} + \sigma_{L23}) + \alpha_T\sigma_T}{\sigma_e + \sigma_n} \qquad (4)$$

where σ_{L1}, σ_{L23}, and σ_T are the partial values of electric conductivity of electrons and holes, respectively; αL and αT are the partial values of the thermopower of electrons and holes.

The diffusion thermopower was determined at various ratios of mobility of electrons and holes and at the relevant simplification $n = p$ and $\frac{\sigma_e}{\sigma_\mu} \approx \frac{\mu}{\nu} = b_{ii}$ by the expression:

$$\alpha = \frac{\alpha_0^h - (\sigma_0^e)b}{1 + b_{ii}}. \qquad (5)$$

In paper [19] it was shown that in the case of two types of carriers and strong degeneration (for Bi this is temperature T < 40 K), partial thermopowers for

quadratic and non-quadratic laws of dispersion are given by the expressions:

$$\alpha_T = (k_B^2\pi^2 T/3e)\left[(r+1)/E_F^T\right] \quad (6)$$

$$\alpha_L = -(k_B^2\pi^2 T/3e)\left[(r+1)\frac{(E_g^L+2E_F)}{E_F(E_g^L+E_F)} - \frac{4}{(E_g^L+2E_F)}\right] \quad (7)$$

where r – scattering parameter of carrier of charge; k_B – Boltzmann constant; E_g^L – energy gap in L point.

As was shown in [19], the electron spectrum in the L point of the Brillouin zone is non-quadratic; the one for holes in the T point of the Brillouin zone may be considered quadratic. Applying expressions (1) for T holes and (2) for L electrons, as well as the scattering factor r_0 = 0.5 (r = 0.5 corresponds to scattering on impurities and takes place in bulk Bi samples at T < 40 K), the value α_{ii} = 1.48 T at $\mu = \nu$ was obtained.

However, even in case of μ/ν = 1, relation (5) does not give quantitative agreement with the experiment, since in this case the maximum value of αii at 40 K is 56 μV/K, not 90–100 μV/K obtained experimentally in pure Bi wires. In addition, the physical cause of non-monotonic dependence $\alpha(T)$ in the whole temperature range 4.2–300 K was not clear.

In work [21] the thermopower for a quantum Bi wire was calculated, taking into account the quantum size effect and the scattering of electrons and holes on long-wave acoustic phonons and rough surface (surface in the form of the δ-like fluctuation).

This mechanism of scattering in quantum structures (films ore wires) was specified in [22, 23].

The peak of the positive polarity $\alpha(T)$ reaches the values of 150–180 μV/K at 30–40 K in Bi-2at%Sb wires with d = 200 nm. The effect of changing the sign of the thermopower in thin wires can be treated in terms of the appearance a new scattering channel stimulated by fluctuations in the diameter d, according to the theoretical works [21–23]. At small diameters d, inevitable fluctuations of the wires diameter Δd lead to the change of the energy carriers at k_{11} = 0. The energy corresponding to the lower subband E is $E = \frac{\pi\hbar^2}{2m^* d^2}$. With increasing the thickness on Δd, this energy is:

$$\Delta E = \frac{\hbar^2\pi^2}{2m^*}\left|\frac{1}{(d+\Delta d)^2} - \frac{1}{d^2}\right| = -\frac{\hbar^2\pi^2}{m^* d^2}\times\frac{\Delta d}{d}\times\frac{1+\Delta d/2d}{(1+\Delta d/d)^2}. \quad (8)$$

Thus, ΔE plays the role of a scattering potential for carriers. The effect of this scattering mechanism will be essential, especially for electrons. This leads to more intense scattering of electrons and to a violation of the relation $\mu >> \upsilon$, (μ, υ are the mobility of electrons and holes, respectively) and to the change in the sign of thermopower on curve $\alpha(T)$.

At low temperatures, when the processes of electron scattering on rough surface are most active due to the quantum size effect, the main contribution to the thermopower is made by holes. Therefore, α is positive and it increases with higher temperature. At further rise of temperature, an appreciable contribution to thermopower is made by the processes of scattering of charged particles on long-wave acoustic oscillations, and the thermopower value begins to be determined by electron scattering on phonons; therefore, the positive contribution to α_{xx} starts decreasing, the thermopower changes its sign and becomes negative. The given model is in good agreement with the presented here experimental results.

From the measured values of the electrical resistivity $R(T)$, the thermopower $\alpha(T)$ (Figs. 7a, 8), the temperature dependence of the Power factor for Bi-2at%Sb wires, various diameters were calculated using the relation P.f. = $\alpha^2\sigma$. The results are shown in Fig. 9. Power factor increases from 300 K up to the maximum for temperatures around 100–70 K and then drops sharply at low temperatures.

Using the value of the thermal conductivity of $\chi_L = 6\cdot10^{-2}$ W/cm·K^2 from [24], the calculated value of the thermoelectric efficiency ZT = 1 is achieved at temperatures of 80–100 K. That makes it possible to use Bi-2at%Sb wires as n-branches in thermoelectric power converters for various purposes. The presence of a glass cover provides them with a high mechanical strength and reliable protection against the environment.

SUMMARY

The single-crystal films and wires on the base of the semimetal alloy $Bi_{1-x}Sb_x$ with different thicknesses and diameters have been investigated. The crystallographic orientation has been reliably established by the X-ray diffraction, the SdH oscillations and angular rotation diagrams of the transverse magnetoresistance. It is shown that the semimetal-semiconductor transition induced by the size quantization in single-crystal semimetal $Bi_{1-x}Sb_x$ films and wires occurs at diameters d, 5–7 times exceeding d in similar structures of pure Bi wires, which allows separating the effects related to the size quantization of the energy spectrum and those of the surface states.

It was found that the appearance and increase of the energy gap ε_g in semimetal Bi-3at%Sb films with

decreasing thickness correlates well with the value of ε_g in semimetallic Bi-2at%Sb wires and reaches the maximum value of 25–30 meV in the wires and films with d = 300 nm.

In semimetal $Bi_{1-x}Sb_x$ films the compressive action of mica and tensile action of polyimide substrates allows manipulating in the semimetal-semiconductor transition in quantum $Bi_{1-x}Sb_x$ films.

It is shown that the maximum value of the thermoelectric figure of merit ZT = 1, at T = 100 K in Bi-2at%Sb wires, which allows using given wires as n-branches in thermoelectric energy converters.

This work was supported by the Moldo-Belarusian project 13.820.05.12/BF. The authors express their gratitude to Mr. Andrzej Karolewski from the International Laboratory of High Magnetic Fields and Low Temperatures for his assistance in the measurements at low temperatures in high magnetic fields.

REFERENCES

1. Yim W.M. and Amith A. Bi-Sb Alloys for Magento-Thermoelectric and Thermomagnetic cooling. *Solid State Electron.* 1972, **15**, 1141.
2. Lenoir B., Dauscher A., Cassart M., Ravich Y.I., Scherrer H. Effect of Antimony Content on the Thermoelectric Figure of Merit of $Bi_{1-x}Sb_x$ Alloys. *J Phys Chem Solids.* 1998, **59**(1), 129.
3. Rowe D.M. *Thermoelectric Handbook: Macro to Nano*. Boca Raton: Taylor & Francis, 2006. 1008 p.
4. Poudel Bed, Hao Qing, Ma Yi, Lan Yucheng, Minnich Austin, Yan Xiao, Wang Dezhi, Muto Andrew, Vashaee Daryoosh, Chen Xiaoyuan, Dresselhaus M.S. High-thermoelectric Performance of Nano-structured Bismuth Antimony Telluride Bulk Alloys. *Science.* 2008, **320**(5876), 634.
5. Ioffe A.F. *Semiconductor Thermoelements, and Thermoelectric Cooling*. London: Infosearch ltd., 1957, 184 p.
6. Hicks L.D. and Dresselhaus M.S. Thermoelectric Figure of Merit of a One-dimensional Conductor. *Phys Rev B.* 1993, **47**, 16631.
7. Lin Y-M, Sun X. and Dresselhaus M.S. Theoretical Investigation of Thermoelectric Transport Properties of Cylindrical Bi Nanowires. *Phys Rev B.* 2000, **62**, 4610.
8. Dresselhaus M.S., Chen G., Tang M.Y., Yang R.G., Lee H., Wang D., Ren Z., Fleurial J.P., and Gogna P. New Directions for Low-Dimensional Thermoelectric Materials. *Adv Mater.* 2007, **19**, 1043.
9. Rabin O., Lin Y.-M. and Dresselhaus M.S. Anomalously High Thermoelectric Figure of Merit in $Bi_{1-x}Sb_x$ Nanowires by Carrier Pocket Alignment. *Appl Phys Lett.* 2001, **79**, 81–83.
10. Hofmann Ph. The Surfaces of Bismuth: Structural and Electronic Properties. *Prog Surf Sci.* 2006, **81**(5), 191.
11. Huber T.E., Adeyeye A., Nikolaeva A., Konopko L., Johnos R.C., and Graf M.J., Huber T.E., Adeyeye A., Nikolaeva A., Konopko L., Johnos R.C., and Graf M.J. Surface State Mobility and Thermopower in Semiconducting Bismuth Nanowires. *Phys Rev B.* 2011, **83**, 2354114.
12. Komnik Y.F., Bukhshtab E., Nikitin Y.V. Specific Features of the Galvanomagnetic Properties of thin Films of Bi"1"–"xSb"x in the Semimetal and Semiconductor Regions. *Thin Solid Films*. 1978, **52**(3), 361–364.
13. Rogacheva E.J. Concentration Anomalies of Properties in Bi–Sb Semimetallic Solid Solutions. *Phys Chem Solids.* 2008, **69**(2–3), 580–584.
14. Rogacheva E., Orlova D.Y.S., Dresslehaus M.S., Tang S. Size Effects in Bi-Sb Solid Solutions thin Films. *Abstr. MRS Fall Meeting 2010, P. LL10.2.* URL: http://www.mrs.org/f10-abstract-ll/
15. Brand N.B., Gitsu D.V., Nikolaeva A.A. and Ponomarev Ya.G. lnvestigation of Size Effects in thin Cylindrical Bismuth Single Crystals in a Magnetic Field. *JETP.* 1977, **45**(6), 1226.
16. Gitsu D., Konopko L., Nikolaeva A. and Huber T. Pressure Dependent Thermopower of Individual Bi Nanowires. *Appl Phys Lett.* 2005, **86**, 10210.
17. Nikolaeva A., Huber T.E., Gitsu D. and Konopko L. Diameter Dependent Thermopower of Bismuth Nanowires. *Phys Rev B.* 2008, **77**, 035422.
18. Грабов В.М., Комаров В.А., Демидов Е.В.., Каблукова Н.С. Заявка на патент: *Способ создания на различных подложках монокристаллических пленок многокомпонентного твердого раствора с равномерным распределением компонентов по объему.* РФ пат. 2012128190/05, 2014. Бюл. № 1.
19. Brandt N.B., Muller R., Ponomarev Ya.G. An Investigation of the Dispersion Law for Carriers in Bismuth Doped with Acceptor-type Impurities. *JETP.* 1976, **44**, 1196.
20. Аскеров В.И. *Кинетические эффекты в полупроводниках*. Л.: Наука, 1970, 303 с.
21. Sinyavskii E.P., Konopko L.A., Nikolaeva A.A., Solovenko V.G., Huber T.E. Research of Thermopower in Quantum Wires. *J of Thermoelectricity*. 2007, **3**, 52.
22. Пшенай-Северин Д.А., Равич Ю.И. Расчет подвижности и термоэлектрической эффективности многослойных структур с квантовыми ямами. *ФТП*. 2002, **36**(8), 974.
23. Nandini Trivedi and Ashcroft N.W. Quantum Size Effects in Transport Properties of Metallic Films. *Phys Rev B.* 1988, **38**(17), 12298.
24. Редько Н.А. Влияние электрон-фононного взаимодействия на фононную теплопроводность полупроводниковых сплавов Bi-Sb. *ФТТ*. 1994, **36**(7), 1978–1993.

Received 09.10.13

Accepted 13.05.14

Реферат

В монокристаллических пленках и нитях висмута происходит переход полуметалл-полупроводник (ПМПП) благодаря эффекту размерного квантования

(ЭРК), который модифицирует фононный спектр, что может представлять практический интерес. Эффект в большей степени может проявляться в наноструктурах на основе сплавов $Bi_{1-x}Sb_x$ в полуметаллической фазе ($x < 0{,}04$), где имеет место минимальное перекрытие L и T зон. В данной статье представлены экспериментальные результаты исследований электронного транспорта, термоэлектрических свойств, осцилляций Шубникова де Гааза (ШдГ) пленок Bi-Sb ($0 < x < 0{,}04$) выращенных термическим напылением в вакууме и нанонитей в стеклянной оболочке, изготовленных усовершенствованным методом Улитовского-Тейлора. Результаты рентгеноструктурного анализа показали, что у монокристаллических пленок тригональная ось ориентирована перпендикулярно плоскости подложки, а одиночные нити Bi-2ат.%Sb с диаметрами 100–1000 нм представляют собой монокристаллы с ориентацией (1011) вдоль оси нити. Исследования ШдГ осцилляций нитей Bi-2ат.%Sb с диаметрами $d > 600$ нм показали, что перекрытие L и T зон в 2 раза меньше, чем в чистом Bi. Температурные зависимости сопротивления $R(T)$ тонких полуметаллических пленок Bi-3ат.%Sb и нитей Bi-2ат.%Sb показывают полупроводниковую зависимость с уменьшением диаметра. Переход (ПМПП), индуцированный размерным квантованием наблюдался при диаметрах почти в 5 раз больших, чем в аналогичных образцах чистого висмута. Этот экспериментальных факт позволяет с одной стороны продвинуться в область более высоких температур (для наблюдения КРЭ), а с другой стороны разделить эффекты, связанные с размерным квантованием и поверхностными состояниями. В полуметаллических пленках $Bi_{1-x}Sb_x$ обнаружено сжимающее действие подложки из слюды, и растягивающее подложки из полиимида в направлении перпендикулярном плоскости пленки, что может служить дополнительным фактором управления переходом (ПМПП). Также обсуждается вопрос термоэлектрических свойств нитей для оптимизации и использования их в термоэлектричестве.

Ключевые слова: нанонити, пленки, переход полуметалл-полупроводник, квантовый размерный эффект, термоэлектричество.